



ITS
Institut
Teknologi
Sepuluh Nopember



Certificate of Appreciation

Number. ID. 015/D/V-ICOME/DTM-ITS/2021

This certificate is awarded to

**I MADE WICAKSANA EKAPUTRA, GUNAWAN DWI
HARYADI, RANDO TUNGGGA DEWA, BUDI
SETYAHANDANA AND SY MINH TUAN HOANG**

as *Authors* of paper

**INVESTIGATION OF PORTEVIN LE-CHATELIER EFFECT
OF AUSTENITIC STAINLESS STEEL 316L(N)
AT HIGH TEMPERATURE REGIMES**

at the 5th International Conference on Mechanical Engineering
25-26TH August 2021



Surabaya, 26TH August 2021




Assoc. Prof. Atok Setiawan

Head of Mechanical Engineering Department
Institut Teknologi Sepuluh Nopember



Achmad Syaifudin, Ph.D

General Chair, Organizing Committee
ICOME 2021



Key Engineering Materials

TP TRANS TECH PUBLICATIONS

Search

SEARCH

Journals

Books

Engineering Research

Advanced Engineering Forum >

Applied Mechanics and Materials >

Engineering Innovations >

Journal of Biomimetics, Biomaterials and Biomedical Engineering >

International Journal of Engineering Research in Africa >

Materials Science

Advanced Materials Research >

Defect and Diffusion Forum >

Diffusion Foundations and Materials Applications >

Journal of Metastable and Nanocrystalline Materials >

Journal of Nano Research >

Key Engineering Materials <

Materials Science Forum >

Nano Hybrids and Composites >

Solid State Phenomena >

Engineering Series

Advances in Science and Technology >

Construction Technologies and Architecture >

Special Book Collections

Foundations of Materials Science and Engineering >

Home » [Key Engineering Materials](#) » Editorial Board



Key Engineering Materials - Editorial Board

ISSN: 1662-9795

Details

Volumes

Editorial Board

Founding Editor

Fred H. Wohlbiert

Editor(s) in Chief

Assoc. Prof. Dr. Cecilia Poletti [SEND MESSAGE](#)

[ORCID](#)

Graz University of Technology, Institute of Materials Science, Joining and Forming; Kopernikusgasse 24/1, Graz, A-8010, Austria;

Prof. Dr. José Manuel Torralba [SEND MESSAGE](#)

[ORCID](#)

Universidad Carlos III de Madrid, IMDEA Materials; Av. Universidad 30, Leganés, 28911, Spain;

Editorial Board

Prof. Aldo Roberto Boccaccini

University of Erlangen-Nürnberg, Institute of Biomaterials, Department of Materials Science and Engineering; Cauerstrasse 6, Erlangen, 91058, Germany;

Prof. Mónica Campos

[ORCID](#)

University Carlos III de Madrid, Department of Materials Science and Engineering; Av. Universidad 30, Leganés-Madrid, 28911, Spain;

Dr. Li Chang

University of Sydney, School of Aerospace, Mechanical and Mechatronic Engineering; Sydney, Australia, 2006;

Prof. Yi Bing Cheng

[ORCID](#)

Monash University, Department of Materials Science and Engineering; PO Box 197, Caulfield East, Australia, 3145;

Prof. Ilaria Cristofolini

[ORCID](#)

University of Trento, Department of Industrial Engineering; Via Sommarive 9, Povo, 38123, Italy;

Prof. Robert Danzer

Montanuniversität Leoben, Institut für Struktur- und Funktionskeramik; Peter-Tunner-Strasse 5, Leoben, A-



Scientific Books Collection

Specialized Collections



Retrospective Collection



Newsletter Subscription

First Name *

Last Name *

Email *

SUBSCRIBE

Subscribe to our Newsletter and get informed about new publication regularly and special discounts for subscribers!

8700, Austria;

Prof. Suong Van Hoa

Concordia University, Department of Mechanical and Industrial Engineering; 1455 Demaisonneuve West # EV 4-145, Montreal, Canada, H3G1M8;

Prof. Xiao Zhi Hu

University of Western Australia, School of Mechanical and Chemical Engineering; Perth, Australia, WA 6009;

Prof. Mohamed A. Taha

Ain-Shms University, Department of Design and Production Engineering, Faculty of Engineering; Khalifa El-Maamon st, Abbasiya sq., Cairo, Egypt, 11566;

Prof. Alejandro Ureña
Fernandez

Universidad Rey Juan Carlos (URJC), Department of Materials Science and Engineering; Tulipan s/n 28933, Mostoles, Madrid, Spain;

Prof. Dragan P. Uskokovic

Institute of Technical Sciences of the Serbian Academy of Sciences and Arts; Knez Mihailova 35/IV, Belgrade, Serbia;

Prof. Maria Teresa Vieira

[ORCID](#)

Universidade de Coimbra, ICEMS - Instituto de Ciência e Engenharia de Materiais e Superfícies ; Pólo II-Pinhal de Marrocos, Coimbra, 3030-788, Portugal;

Prof. Zhi Rui Wang

University of Toronto, Department of Materials Science and Engineering; 184 College Street, Toronto, Canada, M5S 3E4;

Prof. Ming Xing Zhang

University of Queensland, School of Mechanical and Mining Engineering; St. Lucia, Queensland, Australia, QLD 4072;

[DISTRIBUTION & ACCESS](#)

[FOR PUBLICATION](#)

[INSIGHTS](#)

[DOWNLOADS](#)

[ABOUT US](#)

[POLICY & ETHICS](#)

[CONTACT US](#)

[IMPRINT](#)

[PRIVACY POLICY](#)

[SITEMAP](#)

[ALL CONFERENCES](#)

[ALL SPECIAL ISSUES](#)

[ALL NEWS](#)



Scientific.Net is a registered brand of Trans Tech Publications Ltd
© 2023 by Trans Tech Publications Ltd. All Rights Reserved

Table of Contents

Preface

Chapter 1: Metallurgy and Metalworking

Briquetting Pressure Roles in Selective Reduction Process of Limonitic Nickel Laterite F. Abdul, F.G.L.L. Rare, Y. Setiyorini, V.A. Setyowati and S. Pintowantoro	3
Microstructure and Properties of High Frequency Pulse MAG Butt Welded Joints of S355 Steel with Different Diameters X.G. Wu, Z.Y. Zhang, R.Y. Tian, N.Z. Liu, H.C. Tian and C.G. Ding	11
Toughness Recovery of Welded Pipe API 5L Grade B through Quenching and Tempering Treatment V.S. Hadi, F. Mubarak and M. Fitrullah	19
The Portevin-Le Chatelier Type for 316L(N) SS at Low Deformation Rate I.M.W. Ekaputra, G.D. Haryadi, R.T. Dewa, B. Setyahandana and H.S.M. Tuan	25
Mechanical Properties, Microstructural, and Deep Drawing Formability Analysis on the Annealed CuZn35 Brass Alloy for Cartridge Application Widyastuti, R. Rochiem, D.M. Fellicia, C.F.N. Adrinanda and A.P. Wibowo	31
Straightness Geometric Error Assessment for CNC Milling Machine H.B. Harja, A. Nurbaniah, N.S.B. Muhadi and A. Noviandi	39

Chapter 2: Powder Metallurgy

Optimization of Mixing Speed Parameter for Homogeneous Cu-Sn Composite Widyastuti, B.A. Kurniawan, R. Sa'di, N. Safrida and A.P. Wibowo	49
Investigation of the Dwelling Time and Compaction Pressure Effect on Mechanical Properties and Microstructure of the Cu-Sn Composite Widyastuti, R. Fajarin, F. Ali, S.P. Wijaya, E.N. Falah and I. Aditiyawan	57

Chapter 3: Materials and Technologies for Oil and Gas

Effect of the Water Condensation Rate with the Presence of Gas Condensate in the Wet Gas Pipeline H.H. Jarni, W.N.S. Wan Azmi, M.R. Mohd Razlan, A. Md Noor and N. Yaakob	65
Minimizing Adsorption of Anionic Surfactant in Alkaline-Surfactant-Polymer System: Effects of pH and Surfactant Concentration T.A. Tengku Mohd, N.A. Bohairah, M.S. Mat Shayuti, N.K.I. Nik Ab Lah, M.Z. Shahrudin and M.Z. Jaafar	75
Prophecy of Cutting Transport Ratio through a Relationship between Equivalent Circulating Density and Drilled Solid Concentration A. Sauki, P.N.F.M. Khamaruddin, S. Irawan, I. Kinif, S. Ridha, R. Aziz and W.Z. Bakar	83
Comparative Study and Performance Evaluation of Chemical and Biosurfactants in Water-in-Oil Emulsification Process A.M. Som, E.M. Balang and H.A.A. Hamid	93
Optimisation of Rheological Properties of Water-Based Mud (WBM) with Natural Additives by Using Response Surface Methodology (RSM) A.H. Asmungi, N.A. Ghazali, S.F. Abdul Manaf, O.S. Jehan Elham and N.I. Hammizul	103

Chapter 4: Materials for Energy Storage

Reinforced Hydrophobic Molecular Layer Promoting Waterproof Lithium for High-Performance Lithium-Metal Batteries Y.H. Ma	117
--	-----

Regulating Li⁺ Transfer and Solvation Structure via Metal-Organic Framework for Stable Li Anode	
Y.Y. Li, Y. Hu and C.T. Yang	123
A Multi-Functional Artificial Interphase for Dendrite-Free Lithium Deposition	
A.J. Hu and Y.N. Li	129
Surface Coating Modification of Lithium-Rich Manganese-Based Oxide as Cathode Material for Lithium-Ion Batteries	
S.Z. Bu, Y.X. Long, L.B. Zhang, M.Y. Lu, Y.M. Li, D. Wei, Y.P. Xia, Y.M. Luo, S.J. Qiu, F. Xu, L.X. Sun and H.L. Chu	135

Chapter 5: Sustainable Building Materials

Analyse the Effect of Glasswool Roof Insulation Based on the Orientation of the Room to the Sun	
B. Yanto, C.L. Lim, C.S. Hassan and S. Shahul	145
Natural Hydraulic Lime Mortars for Hot-Humid Climates: Effects of Oyster Shells as Seeding Compound	
N. Razali, A.M. Forster, N. Razali and N. Jumadi	159
The Effects of Chicken Eggshell Powder as Fine Aggregate Replacement on Mortar Pore Structure	
N. Razali, N. Jumadi, N. Razali and Y. Lazim	171
Spent Garnet and Concrete	
R. Samsunanwar, H.F. Rebzuwan and A. Md Som	187

The Portevin-Le Chatelier Type for 316L(N) SS at Low Deformation Rate

I.M.W. Ekaputra^{1,a*}, Gunawan Dwi Haryadi^{2,b}, Rando Tungga Dewa^{3,c},
Budi Setyahandana^{1,d} and Sy Minh Tuan Hoang^{4,e}

¹Universitas Sanata Dharma, Paingan, Maguwoharjo, Depok, Sleman-Yogyakarta 55282, Indonesia

²Universitas Diponegoro, Jl. Prof. Sudharto, SH., Tembalang-Semarang 50275, Indonesia

³Universitas Pertahanan, Kawasan IPSC Sentul, Bogor-Jawa Barat, 16810, Indonesia

⁴Thu Dau Mot University, 6. Tran Van On. Phu Hoa Ward, Thu Dau Mot City, Binh Duong, 820000, Vietnam

^amade@usd.ac.id, ^bgunawan_dh@ft.undip.ac.id, ^crando.dewa@idu.ac.id, ^dbudisetya@usd.ac.id, ^ehoangsyminhtuan@tdmu.edu.vn

Keywords: Austenitic stainless steel 316L(N), Portevin Le-Chatelier, Work hardening

Abstract. This study determined the serrated yielding type for 316L(N) SS due to the Portevin-Le Chatelier effect under particular temperature conditions with the range of 24 to 655 °C at 10⁻⁵/s of plastic deformation rate. The 316L(N) SS was loaded by tensile test apparatus equipped with a three-zone furnace. The cylindrical specimen was put at the centre of the furnace. Since the test was conducted at various temperatures, a thermocouple was attached to the surface of the specimen. After the test, the engineering stress-strain curve was plotted, and the serrated yielding was observed. The results showed that the type A, B, D, and E were identified for a particular temperature. Type B was identified at the low-temperature region, and type A was identified at the high-temperature region. In addition, the work hardening rate curve was plotted to describe the plastic deformation characteristic.

Introduction

Strain rate sensitivity is one of the critical parameters that must be considered to determine the creep deformation mechanism [1]. The wide range of strain rates can lead to the change of flow stress. The three-stage in the creep curve occurred due to the alteration of strain rate value. An incremental change of strain rate occurred during the first stage, where the work hardening developed. A constant strain rate occurred at the second stage, where the recovery and hardening process was relatively balanced. The last stage is the rupture process, where the strain rate incrementally increase. It has been reported that at a particular strain rate value, the heterogeneous plastic deformation or also known as the Portevin Le-Chatelier effect, can lead to a loss in ductility and produce a rippled surface [2,3]. Macroscopically, the heterogeneous plastic deformation has been modelled by a well-known model, namely dynamic strain ageing (DSA). The DSA can be simply modelled when the solute atom experienced an ageing process [3-5]. The ageing process occurred since the mobile dislocation was impeded by an obstacle such as Forrest and pipe dislocation [4,5].

The serrated yielding phenomenon has been investigated for several metal alloys such as aluminum alloy, stainless steel, and nickel-based super-alloys [2,4-8]. The 316L(N) SS as one type of austenitic stainless steel is still an essential component for the power plant [5, 9-11]. This type of steel has several unique properties, exceptionally compatible with the liquid sodium coolant and stable at elevated temperatures. Several studies have been conducted to investigate the characteristic of 316L(N) SS under tension load for particular temperature and strain rate conditions [11]. Furthermore, it has been reported that uncommon due to serrated yielding was found for particular strain rate and temperature. Since this steel grade is still in use, more information about the serrated yielding for a wide range of temperature and strain rates is still required.

In this study, the 316L(N) SS was investigated at elevated temperature and $10^{-5}/s$ of deformation rate. The tension test was conducted in the temperature ranges of 24 °C - 655 °C. By plotting the engineering stress-strain curve, the serrated yielding was observed and identified. In addition, to investigate the strain rate effect on the plastic deformation process, the work hardening curve was plotted and discussed.

Experimental Procedure

In this study, the naming of “L(N)” is defined that this steel grade has a particular amount of Nitrogen (0.1 wt.%) and Carbon (< 0.03 wt.%). This 316L(N) SS has 0.020C–1.05Mn–0.0027P–0.005S–17.1Cr–2.4Mo–12.2Ni–0.08N (wt.%). The ingot was normalized before being formed into a cylindrical form. Specimen size and dimensions followed the manufactured into a cylindrical specimen ASTM E8 [12]. The cylindrical specimen has a circular diameter of 6 ± 0.01 mm and a gauge length of 30 ± 0.01 mm. The specimen was intended to have a smaller diameter around the centre to produce a fracture at the centre position. All specimens were cut in the rolling direction and polished with #2000 of sandpaper grit. The specimen size and dimension were shown in Fig. 1.

The strain rate was controlled by setting the constant crosshead velocity of $10^{-5}/s$. Since the tensile test was conducted at elevated temperatures, the test followed the ASTM E21 [13]. The three-zone heating furnace was applied for the test at elevated temperature. The cylindrical specimen was put at the centre of the furnace and attached with a thermocouple on the specimen surface. Before loading the specimen, the furnace was heated until reaching the destination temperature with the range within ± 3 °C. A universal testing machine with a capacity of 50 kN was applied for the tensile test. Since no extensometer was not be used, the specimen elongation was measured based on the displacement of the crosshead movement.

Results and Discussion

The tensile test result for 316L(N) SS with the range of 24 to 655 °C at $10^{-5}/s$ was represented by the engineering stress-strain curve in Fig. 2. It can be seen that the curve trend is decreasing with an increase in temperatures. The ultimate tensile strength and yield strength decrease significantly above room temperature. The recovery takes control with the higher temperatures. It is also seen that the curves are located at the narrow band for the temperature range of 190 °C - 655 °C. It has been reported that the narrow band indicated the serrated yielding occurrence [5]. The serrated yielding can also be seen at the non-linear curve (plastic area) in the engineering stress-strain curve where work hardening has occurred. From literature, the serrated yielding does typically not found at room temperature [5,11]. However, the serrated yielding is found for 316L(N) SS at 24 °C with $10^{-5}/s$ of strain rate.

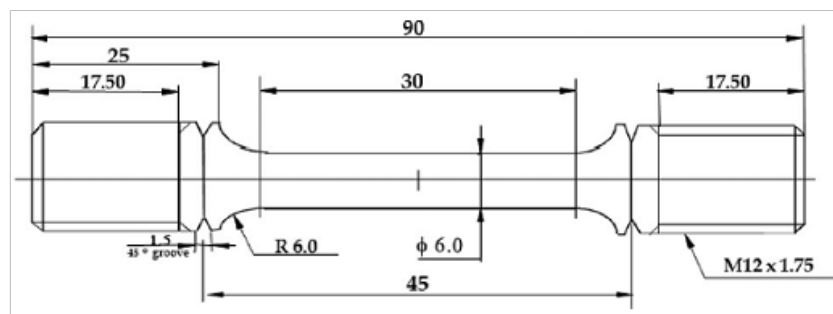


Fig. 1. Specimen size and dimesion for the tensile test.

Fig. 3 shows the magnification of the plastic curve for each temperature condition. It is seen that the different type of serrated yielding is formed. The type of serrated yielding is summarized in Table 1. Type B is observed at the range of 24 °C - 290 °C. Type B is indicated by the load oscillation about the centre of the stress-strain curve. Following the classical DSA theory, the oscillation occurred since

the ageing time of the solute atom was short [14]. Therefore, the mobile dislocation moved with high diffusivity. Type A is observed at the range of 335 °C - 440 °C. Type A is indicated by the sudden increase of load followed by load drop to the centre of the stress-strain curve. Type A is almost the same as type B, with the lower diffusivity of mobile dislocation due to the longer ageing time. The combination of type A+E is observed at the range of 510 °C - 545 °C. Type E typically appears at higher stress and higher temperature after type A. Type D is observed at 610 °C. Type D indicates the plateaus on the stress-strain curve. The combination of type A+B is observed at 655 °C.

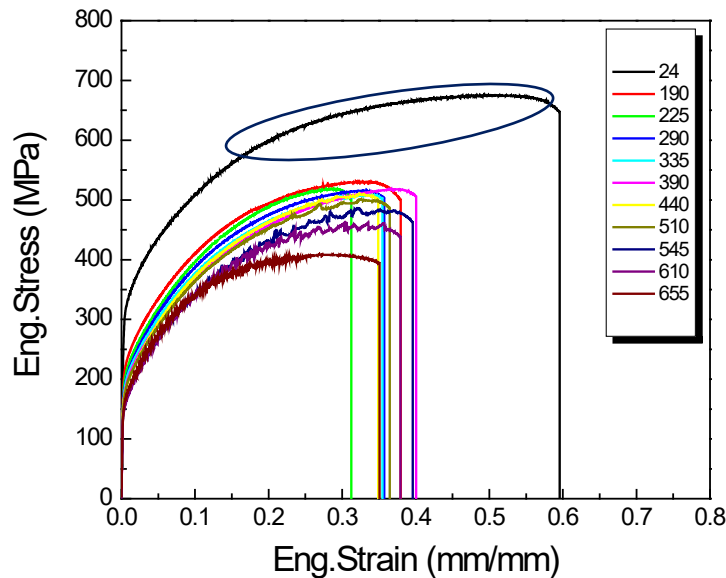
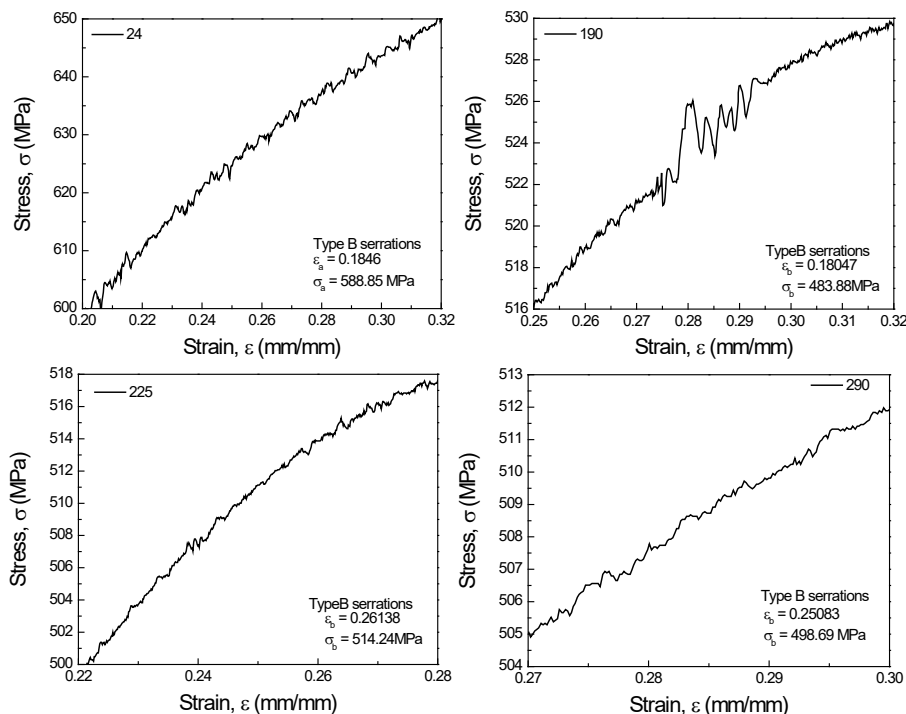


Fig. 2. Engineering stress-strain curve of 316L(N) SS.



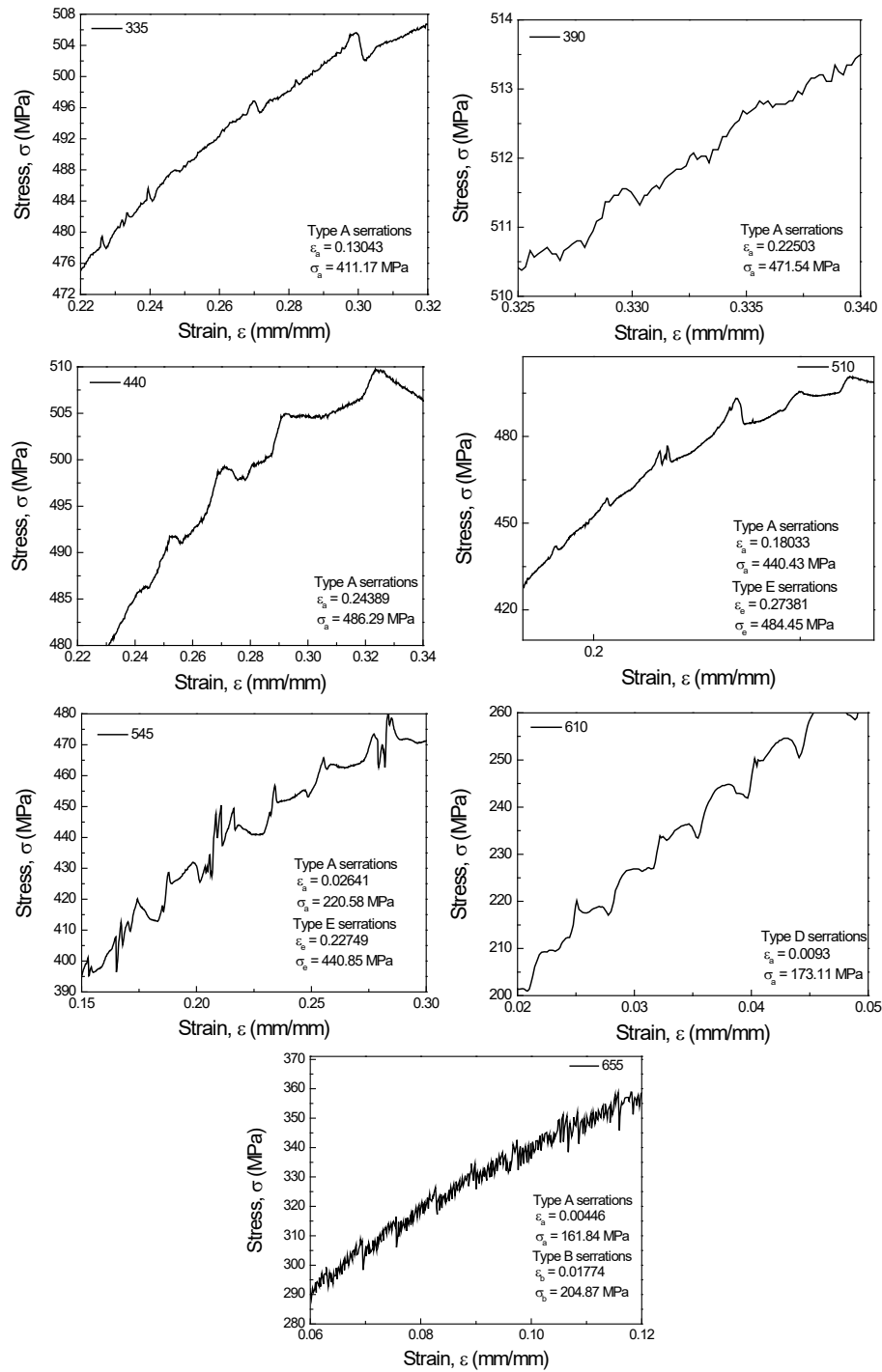


Fig. 3. Type of serration yield for each temperature condition.

Table 1. Identification of serrated yielding type for 316L(N)SS.

	24	190	225	290	335	390	440	510	545	610	655
A	-	-	-	-	O	O	O	O	O	-	O
B	O	O	O	O	-	-	-	-	-	-	O
C	-	-	-	-	-	-	-	-	-	-	-
D	-	-	-	-	-	-	-	-	-	O	-
E	-	-	-	-	-	-	-	O	O	-	-

The curve of work hardening rate of 316L(N) SS under various temperatures at $10^{-5}/s$ is represented in Fig. 4. In this study, the work hardening rate for 316L(N) SS confirmed the previous study obtained by Samuel [15]. The work hardening rate, θ , is determined by calculating the derivative of true stress, σ_t , to the true strain, ϵ_t [14]. the three stages of work hardening rate was seen

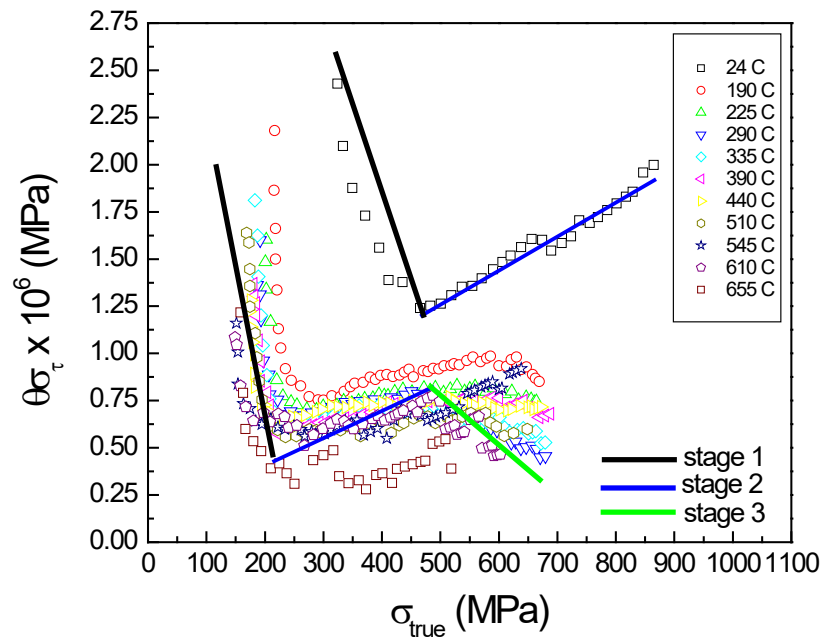


Fig. 4. Work hardening rate for 316L(N) SS at $10^{-5}/s$.

by plotting $\theta\sigma_t$ vs σ_t . The first stage was initially indicated by a rapid decrease in $\theta\sigma_t$ followed by a gradual increase in $\theta\sigma_t$. The first stage is also called a transient stage, interpreted as plastic strain increases due to increasing mobile dislocation density after passing the elastic limit. The second stage was related to the hardening process where the slip was activated and resulted in heterogeneous dislocation. Finally, the third stage was identified as the recovery process.

Summary

In this preliminary study revealed that the serrated yielding type for 316L(N) SS was dominated by types A and B under various temperatures at $10^{-5}/s$. The remaining type of serrated yielding was also observed as type D and E. Following the engineering stress-strain curve, the work hardening rate showed that the recovery process was not found at room temperature. While above the room temperature, the recovery process occurred after the hardening process.

References

- [1] A. K. Gosh, On the measurement of strain-rate sensitivity for deformation mechanism in conventional and ultra-fine grain alloys, *Mater. Sci. Eng. A.* 463 (2007) 36–40.
- [2] S. Tamimi, A. Andrade-Campos, J. Pinho-da-Cruz, Modelling the Portevin-Le Chatelier effects in aluminium alloys: a review, *J. Mech. Behav. Mater.* 24 (3–4) (2015) 67–78.
- [3] R. C. Picu, A mechanism for the negative strain-rate sensitivity of dilute solid solutions, *Acta Mater.* 52 (2004) 3447–3458.
- [4] H. Ovri, E. T. Lilleodden, New insights into plastic instability in precipitation strengthened Al–Li alloys, *Acta Mater.* 89 (2015) 88–97.
- [5] I. M. W. Ekaputra, W. G. Kim, J. Y. Park, S. J. Kim, E. S. Kim, Influence of dynamic strain aging on tensile deformation behavior of alloy 617, *Nucl. Eng. Technol.* 48 (2016) 1387–1395.
- [6] H. Halim, D. S. Wilkinson, M. Niewczas, The Portevin–Le Chatelier (PLC) effect and shear band formation in an AA5754 alloy, *Acta Mater.* 55 (2007) 4151–4160.

-
- [7] K. K. Alaneme, M. O. Bodunrin, E. A. Okotete, On the nanomechanical properties and local strain rate sensitivity of selected aluminium based composites reinforced with metallic and ceramic particles. *J. King Saud Univ. Eng. Sci.* (2021).
- [8] S. Yang, L. Xue, W. Lu, X. Ling, Experimental study on the mechanical strength and dynamic strain aging of Inconel 617 using small punch test, *J. Alloys Compd.* 815 (2020) 1–8.
- [9] H. D. Kweon, J. W. Kim, O. Song, D. Oh, Determination of true stress-strain curve of type 304 and 316 stainless steels using a typical tensile test and finite element analysis, *Nucl. Eng. Technol.* 53 (2021) 647–656.
- [10] X. Sun, R. Xing, W. Yu, X. Chen, Uniaxial ratcheting deformation of 316LN stainless steel with dynamic strain aging: experiments and simulation. *Int. J. Solids Struct.* 207(15) (2020) 196–205.
- [11] D. R. Palaparti, V. Ganesan, J. Christopher, G. P. V. Reddy, Tensile flow analysis of austenitic type 316LN stainless steel: effect of nitrogen content. *J. Mater. Eng. Perform.* 3 (2021).
- [12] ASTM E8 / E8M-21, Standard Test Methods for Tension Testing of Metallic Materials, ASTM International, West Conshohocken, PA (2021).
- [13] ASTM E21-20, Standard Test Methods for Elevated Temperature Tension Tests of Metallic Materials, ASTM International, West Conshohocken, PA (2020).
- [14] P. Rodriguez, Serrated plastic flow. *Bull. Mater. Sci.* 6 (1984) 653–663.
- [15] E. I. Samuel, B. K. Choudary, K. B. S. Rao, Influence of temperature and strain rate on tensile work hardening behaviour of type 316 LN austenitic stainless steel. *Scr. Mater.* 46 (2002) 507–512.